Effect of Fluid Flow, Solution Chemistry and Surface Morphology of Fibrous Material on Colloid Filtration

Manoj Dagaonkar, Ph.D., Udayan Majumdar

Hindustan Unilever Limited, Bangalore, Karnataka INDIA

Correspondence to:
Manoj Dagaonkar email: manoj.dagaonkar@unilever.com

ABSTRACT

The goal of this paper is to focus on the effect of fluid flow, solution chemistry and surface morphology of fibrous media (in terms of roughness and charge heterogeneity) on colloid removal. A theoretical framework on the role of flow velocity on particle deposition to cylindrical substrate is presented. Existing theories related to particle attachment onto cylindrical substrates and on the effect of surface morphology on better predictability of particle adhesion have been modified. At higher flow velocities, the theory predicted the detachment of larger sized particles from the collector surface owing to the increased lift forces. Experimental studies confirmed removal of 3 μ particles at higher flow velocities. The effect of solution chemistry (in terms of concentration and ionic strength) on the particle adhesion has been studied. The ionic strength improved the attachment of the microspheres, despite the presence of high energy barriers as predicted by DLVO calculations. A new model incorporating the surface roughness and charge heterogeneity was developed that predicted a reduction in the energy barriers in otherwise unfavorable conditions of adhesion, and hence could explain the adhesion more accurately than DLVO alone.

Keywords: colloid deposition, depth filtration, particle transport, DLVO, surface roughness, charge heterogeneity.

INTRODUCTION

Granular and fibrous bed filtration is the most commonly used engineering practices for the removal of suspended particles and microbes of various kinds from a fluid flow. The filtration bed is used as a means for investigating colloidal interactions with the collector surface. The capture of such particles and microbes is governed by several mechanisms depending upon the particle size, flow conditions (hydrodynamics), physico-chemical properties of the particles and the collector and the solution chemistry. A thorough understanding of filtration is essential for predicting the transport and fate of the particles within the bed of collectors.

From the study of the deposition of model colloids on well-defined solid surfaces, it is well known that deposition involves two sequential steps: transport and attachment. The transport of colloidal particles from the fluid to the vicinity of a filter grain (collector) is typically described by three mechanisms: interception, gravitational sedimentation and Brownian diffusion [1, 2]. The attachment of the particles is controlled by colloidal interaction forces which operate at short distances of separation. These colloidal interactions include electrical double layer and van der Waals interactions, hydrodynamic interactions, hydration (structural) forces, hydrophobic interactions for hydrophobic surfaces, and macromolecular adsorbed layer (steric) interactions when macromolecules or polymers are adsorbed onto the interfaces of interacting particles and collectors. The sum of the colloidal interactions (the van der Waals and electrical double layer) yields the total interaction energy which forms the basis of the Derjaguin-Landau and Verwey-Overbeek (DLVO) theory of colloid stability [3]. The interaction depends on the size of the particles and the collector, net charge on the particle and the collector, the separation distance between the particle and the collector, the Hamaker constant of the interacting media, the electrolyte concentration and the valence of the counter ion. In addition to these interactions, the surface roughness of the particles and collectors, charge heterogeneity, and the particle deposition in the secondary minima contribute to the particle adhesion and cannot be explained by DLVO theory.

The kinetics of the capture (attachment) of colloids is determined by the magnitude of the colloidal interactions between the particles and collectors.

These interactions are controlled by the chemical characteristics of the solid-solution interface of colloids and collectors and by the solution chemistry. The critical role of the solution chemistry and colloid interactions in the attachment step is poorly understood.

The single collector contact efficiency in a clean bed is the rate of deposition onto the collector to the rate at which the particles flow towards the projected area of the collector.

The performance of a packed bed is related to the efficiency of a single spherical collector by: [4-6]

$$\frac{dC}{dL} = -\frac{3}{2}\frac{(1-f)}{d}\alpha\eta C \qquad (1)$$

where f is the bed porosity, L is the bed depth and α is the collision efficiency factor (sticking coefficient) which reflects the chemistry of the system. Integrating Eq. (1),

$$\ln\left(\frac{C}{C_0}\right) = -\frac{3}{2}\frac{(1-f)}{d}\alpha\eta L \qquad (2)$$

where C_0 and C are the influent and effluent concentrations for the packed bed.

As more and more particles stick to the collector surface, some of the previously deposited particles also act as additional collectors and allow other particles to stick to them. Hence, for the case when the actual collector consists of a filter grain and an associated number of particles attached to it that act as collectors, the combined contact efficiency is equal to the ratio of the sum of the rate at which particles strike the filter grain and retained particles to the rate at which particles flow towards the collector (with the retained particles). Out of all the particles which strike the collector, there are only a few that stick or get attached onto the collector surface. The sticking coefficient (or attachment efficiency) is defined as the rate at which the particles stick to the collector surface to the rate at which the particles strike the collector. The dimensionless deposition (or removal) rate of the particles is the product of the contact efficiency and the sticking coefficient.

The attachment efficiency accounts for the chemical-colloidal effects on the rate of deposition while the contact efficiency accounts for the physical effects. Thus, when the chemical-colloidal interactions are favorable for deposition (i.e., in the absence of repulsive total energy of the interaction energies), the attachment efficiency approaches unity and the deposition rate is equal to the transport rate. In this case, the particle transport is the rate determining step and is referred to as a favorable deposition. When chemical-colloidal interactions are unfavorable for deposition (i.e., repulsive colloidal interactions predominate), the attachment efficiency is smaller than one and the particle deposition rates are hindered. This case is referred to as unfavorable deposition.

The cylindrical shaped collectors, having more surface area to volume ratio, can remove particles more efficiently compared to the spherical collectors. The existing theory on particle detachment does not take into consideration the role of lift force on the attachment. Also, it does not predict the influence of flow velocities on the particle adhesion.

This paper focuses on the effect of the following parameters on colloid filtration:

(a) Fluid flow dynamics
(b) Solution chemistry
(c) Surface morphology of fibrous materials in terms of roughness and heterogeneity.

A modified equation on particle adhesion has been presented to predict the particle attachment for a wider size distribution at different flow velocities. This equation predicts the flow conditions beyond which particle detachment occurs. The theory has been validated with experiments at various flow velocities. The role of solution chemistry and colloid concentration of 3 μ model particles on the removal efficiency is studied (using flow conditions predicted from the particle adhesion theory). To predict a more accurate removal of the particles at various salt concentrations, a theoretical understanding on the role of the surface morphology and charge heterogeneity has been discussed.

THEORETICAL CONSIDERATIONS

Particle Deposition

The retention of the particles in the filter bed requires that the adhesion force between a retained particle and the collector is in equilibrium with the hydrodynamic force which tends to detach the particle. Particle detachment in filtration, therefore, occurs only when the hydrodynamic force overcomes the adhesive force. The mechanisms of the particle detachment from the collector include rolling, sliding and lifting [7].

In a fibrous collector-type deep bed filtration, the fiber length is significantly larger than the colloidal particles being removed. The main forces acting on the particle separated with a distance δ from the collector are the London-van der Waals force, F_L, in the direction normal to the collector plane; electrical double layer force, F_D, in the direction normal to the collector plane; hydrodynamic drag force, F_d, due to the fluid flow in the tangential direction along the collector plane; and hydrodynamic lift force, F_l, in the direction normal to the collector plane.

If the attached particle tends to be re-entrained due to the fluid flow, a frictional force F_F arises in the direction opposite to that of F_d to prevent the re-entrainment. The basic assumption is that if $F_F < F_d$, the lifting force F_l would then cause the particle to drift away from the collector and so particle detachment or dislodging in the filter takes place. F_L, F_D and F_l are the forces responsible for particle adhesion. The other forces include the gravity force F_G in the vertically downward direction along with the flow direction, the buoyancy force F_B in the vertically upward direction and the Brownian force exerted due to particle collisions with the surrounding fluid molecules.

Adhesion Forces

The adhesion forces are given as [7]:

$$F_L = \frac{1}{12}\frac{H d_p^3}{\delta^2 (\delta + d_p)^2} \tag{3}$$

$$F_D = \left(\frac{2\pi\varepsilon\varepsilon_0 r_p \zeta_P^2 + \zeta_g^2) k e^{-k\delta}}{1 - e^{-2k\delta}}\right) \times \left(\frac{2\zeta_p \zeta_g}{\zeta_P^2 + \zeta_g^2} - e^{-k\delta}\right) \tag{4}$$

where H is the Hamaker constant, δ is the separation distance between the particle and the collector plane, ε_0 is the dielectric constant (permittivity) in vacuum, ε is the relative dielectric constant of the fluid, ζ_p and ζ_g are the zeta potentials of the particle and the collector, respectively. k is the Debye reciprocal double layer thickness which is given as:

$$k = \left(\frac{e^2 \sum n_{i\infty} z_i^2}{\varepsilon\varepsilon_0 k_B T}\right)^{1/2} \tag{5}$$

where $n_{i\infty}$ is the bulk number density of ions in a solution, k_B is Boltzmann's constant, T is the absolute temperature, e is the charge of the electron and z is the valence of the ion species.

Hydrodynamic Forces

The hydrodynamic drag force on a spherical particle of diameter d_p and for Re < 1 can be calculated as [7, 8]:

$$F_d = \frac{3\pi\mu d_p u_p}{\xi} \tag{6}$$

where μ is the fluid viscosity, u_p is the particle velocity and ξ is the non-dimensional gap defined as ratio of separation distance between the particle and the collector and the particle radius. For gap widths much smaller than the particle radius, the hydrodynamic drag force has a correction for lubrication resistance. This equation indicates that the drag force has a higher magnitude for a fluid with higher viscosity and for larger particles. As the particle velocity increases, the resistance to motion increases resulting in a higher magnitude of the drag force.

The hydrodynamic lifting force for a single sphere in an unbounded linear shear flow is written as [7]:

$$F_l = 0.761 \frac{\tau_w^{1.5} d_p^3 \rho^{0.5}}{\mu} \tag{7}$$

τ_w is the shear stress acting on the collector as is expressed as:

$$\tau_w = 3\mu \frac{A_s}{d} u \tag{8}$$

where A_s is defined as $2(1 - p^5)/w$, $w = 2 - 3p + 3p^5 - 2p^6$, $p = (1-f)^{1/3}$, u is the approach fluid velocity.

The lift force is always perpendicular to the drag force caused by that velocity. Its magnitude with respect to the normal drag force will play an important role in the deposition of the particles. The lift force also depends on the particle size. The higher the particle size, then the greater is the lift force.

Detachment Forces

The friction force is responsible for the particle detachment, in case it is not sufficient to overcome the drag. The force with which the particle comes out due to this imbalance is deemed the lift force. This force is assumed to be proportional to the adhesive force by [7]:

$$F_F = k_f \; F_L = k_f' \, S \, F_L = k_f' \, \frac{6(1-f)}{d} F_L \qquad (9)$$

where k_f is the coefficient of sliding friction, k'_f is the proportionality constant, S is the specific surface area of the deep bed filter, defined as the surface area per unit filter bed volume, and d is the collector diameter.

If the frictional force is smaller than the drag force, the lifting force would cause the particle to drift away from the collector and so particle detachment or dislodging in the filter can occur. The lift force is a strong function of the flow velocity of the fluid. Specifically, at high fluid flow velocities, the contribution of the lift force is expected to be higher. The existing literature does not consider the role of the lift force on particle adhesion. Hence, the modified net adhesion force for the particle attachment onto the collector surface can be given as:

$$F_{Adh} = F_L - F_D - F_l \qquad (10)$$

Hence there will be particle adhesion when $F_{Adh} > 0$.

Energy of Interaction

The theoretical potential energy of interaction, E_{DLVO}, between the particle and the collector can be calculated using DLVO theory. A cylindrical collector and the particle are modeled as a flat plate and sphere, respectively, [8] and the energy of interaction is written as:

$$E_{DLVO} = E_{vdw} + E_{EDL} \qquad (11)$$

where E_{vdw} is the interaction potential due to van der Waals forces and E_{EDL} is the interaction potential due to electrical double layer repulsion force. E_{vdw} is determined as:

$$E_{vdw} = \frac{-H}{6}\left[\frac{r_p}{\delta} + \frac{r_p}{\delta + 2r_p} + \ln\left(\frac{\delta}{\delta + 2r_p}\right)\right] \qquad (12)$$

E_{EDL} is given by the Wiese and Healy expression for a sphere-plate system as:

$$E_{EDL} = \left(2\pi r_p \, n_{i\infty} \, k_B T \, \frac{\varphi_1^2 + \varphi_2^2}{k^2}\right) \times \left[\frac{2\varphi_1\varphi_2}{\varphi_1^2 + \varphi_2^2} \ln\left(\frac{1+e^{-k\delta}}{1-e^{-k\delta}}\right) + \ln(1-e^{-2k\delta})\right] \qquad (13)$$

$$\varphi_i = \frac{z\, e\, \zeta_i}{k_B T} \qquad (14)$$

where H is the Hamaker constant for the system collector-water-particle, r_p is the particle radius, φ is the reduced potential of either the collector or the particle, and ζ is the surface potential as determined by the streaming potential for the collector or the particle. Eq. (13) is valid for systems with minimal electrical double-layer distortion ($k\, r_p >> 1$) where $\delta << r_p$ and for small surface potentials, ζ.

A common feature for most of the earlier models (including the DLVO model) was the assumption that the surfaces of the collectors and the particles are ideal, meaning that the important chemical and physical properties of the surface were uniform everywhere. Specifically, the surfaces are assumed perfectly smooth with a uniform surface charge density. It is widely recognized that the surfaces are heterogeneous and that the degree of heterogeneity present on typical surfaces can be sufficient to alter the colloidal forces between them. [9-11] When the conditions for deposition are favorable, meaning that no energy barrier to deposition exists, the deposition rate can be predicted relatively accurately. On the other hand, if the energy barrier exists between the particle and the collector surface, the rate of particle deposition has been found to be greater than predicted. In nearly all such cases, surface heterogeneity in terms of the surface roughness and non-uniform charge density was listed as a possible cause. Many new equations and theories have been put forward in the recent past [9-17] to explain the effect of these parameters on the particle attachment efficiency.

Recent models are based on an approach where the asperities are assumed to be hemispherical caps on a smooth surface of the collector. A simple approach to assess the effect of the surface roughness on the total interaction energy and the collision efficiency was stated in the literature [9]. The roughness was due to the small half-spheres protruding from the surfaces of the particles and collectors. For the case of a smooth sphere interacting with a rough spherical collector, the interaction energy was calculated from the sum of the particle-half sphere protrusion interaction and the particle smooth collector interaction. The closest distance between the particles and the collector was determined by the size of the protrusions on the surface of the collector. The total interaction energy

as a function of the separation distance (δ) between a single particle and a single half-sphere protrusion of radius r_a was given as:

$$E_T(\delta) = E(\delta) + E(\delta + r_a) \quad (15)$$

Similar to this, for a spherical particle interacting with a surface with asperity, the force of the adhesion on the surface can be written as a combination of sphere-sphere and sphere-surface interactions in the form of [12]:

$$F_{adh} = \frac{H\, r_p}{6\delta^2}\left[\frac{r_a}{r_a + r_p} + \frac{1}{(1 + y_{\max}/\delta)^2}\right] \quad (16)$$

where H is the Hamaker constant, r_p is the particle radius, δ is the equilibrium distance of separation, r_a if the radius of asperity, y_{max} is the height of asperity.

For a spherical particle approaching a collector with a single protrusion, the adhesive force balance equation can be written as [13]:

$$F_{adh} = \frac{H\, r_p}{6\delta^2}\left(\left(\frac{1}{1 + r_p/(1.485\, r_a)}\right) + \left(\frac{1}{(1 + 1.485\, r_a/\delta)^2}\right)\right) \quad (17)$$

where 1.485 r_a is the radius of spherical asperity and r_a is the root mean square roughness of the collector surface.

For the contact between a flat particle and the surface with hemispherical asperity, the adhesive force is the sum of interaction between the asperity and the flat surface and the non-contact interaction from the two parallel plates of area A and is expressed as [14]:

$$F_{adh} = \frac{H}{6\delta^2}\left[r_a + \frac{A}{\pi\,\delta(1 + y_{\max}/\delta)^3}\right] \quad (18)$$

In addition to these, equations have been reported for asperities, within the particle and flat collector surfaces [15, 16], and these equations are limited to perfectly smooth surfaces.

While the literature focuses on asperities in terms of protrusions, collectors can have asperities in terms of valleys. Hence, the new proposed equation for a spherical particle approaching a single collector having a single protrusion and a single valley can be written as a summation of the adhesive forces between particle-protrusion, particle-valley and particle-plane surface as written below:

$$F_{adh} = \frac{H\, r_p}{6}\left[\left(\frac{r_a}{r_a + r_p}\right)\frac{1}{(\delta - r_a)^2} + \left(\frac{1}{(\delta + r_a)^2}\right) + \left(\frac{1}{\delta^2}\right)\right] \quad (19)$$

Integrating Eq. (19),

$$E_{vdw} = \int_{\infty}^{\delta} F_{adh}\, d\delta \quad (20)$$

If the rms roughness of the collector surface is known, then the radius of the hemispherical asperity for the collector is expressed as [14]:

$$r_a = 1.485 \text{ rms} \quad (21)$$

Substituting the value for r_a in Eq. (20), the energy of the interaction (van der Waals interaction energy) can be calculated by the new proposed equation as:

$$E_{vdw} = \frac{-H\, r_p}{6}\left[\left(\frac{1.485\, r_a}{1.485\, r_a + r_p}\right)\frac{1}{\delta} + \left(\frac{1}{\delta + 1.485\, r_a}\right) + \left(\frac{1}{\delta + 2 \times 1.485 \times r_a}\right)\right] \quad (22)$$

Other than the surface roughness, the other important parameter, which is equally as important, is the surface charge heterogeneity of the collector. The equation for the potential energy between two non-uniformly charged spheres is expressed as [17]:

$$E_{EDL} = \frac{\pi\,\varepsilon\,\varepsilon_0\, r_p\, r_c}{r_p + r_c}\left[\begin{array}{l}(\zeta_A^2 + \zeta_B^2 + \sigma_A^2 + \sigma_B^2) \times \\ \ln(1 - e^{-2k\delta}) + \\ 2\zeta_A\,\zeta_B \times \\ \ln\left(\frac{1 + e^{-k\delta}}{1 - e^{-k\delta}}\right)\end{array}\right] \quad (23)$$

For a spherical particle approaching a cylindrical collector, the collector plane radius >> radius of the particle, hence, Eq. (23) can be modified as:

$$E_{EDL} = \pi \varepsilon \varepsilon_0 \; r_p \left[\begin{array}{l} (\zeta_A^2 + \zeta_B^2 + \sigma_A^2 + \sigma_B^2) \times \\ \ln(1 - e^{-2k\delta}) + \\ 2\zeta_A \zeta_B \; \ln\left(\dfrac{1+e^{-k\delta}}{1-e^{-k\delta}}\right) \end{array} \right] \qquad (24)$$

Eq. (22) and Eq. (24) are used to predict the interaction energy profiles for the collector with surface roughness and charge heterogeneity to explain the deviation from DLVO theory.

MATERIALS AND METHODS

Materials

The Whatman filter paper with a Grade 4, having a pore size in the range of 20-25 µm, was procured from Acerasayan, Bangalore, India. Nonwoven polyester fabric with a weight of 500 g/m^2 and a thickness of 2 mm was procured from Travencore Fibers Private Limited, Mumbai, India. Mono-disperse fluorescent latex microspheres were purchased from Polysciences Inc. as a 2.5 wt% aqueous suspension (~ 1.68 x 10^9 microspheres/ml) and were stored in the dark at 4^{0}C and were used as model particles. The fluorescent microspheres are comprised of non-carboxylated polystyrene particles of 3 µm size. LR grade sodium chloride, sodium bicarbonate and calcium chloride dehydrate were procured from Merck Limited, Mumbai, India.

METHODS

Preparation of Model Water

Model water 1 was prepared by adding the required amounts of calcium chloride or sodium chloride and mono-dispersed latex microspheres (at a concentration of ~ 50000/L) to de-ionized (DI) water. This water was prepared to study the effect of the ionic strength on the removal of the microspheres and had a turbidity of ~ 0.5-1 NTU. For adjusting the water pH, NaOH or HCl was used. Microspheres have been widely used in the literature as model particles as they are available in various accurate sizes.

Model water 2 was prepared by adding different amounts of microspheres to the DI water with different levels of sodium chloride or calcium chloride (10-5000 ppm). This water was prepared to study the effect of the concentration of the microspheres on the removal and had a turbidity of ~ 0.5-1 NTU and pH of 7 (adjusted by NaOH or HCl)). This water represents a wider range of water quality in terms of its ionic strength and colloidal concentration.

Filtration Experiments

The Tarson's filtration unit was used to study the microsphere removal. The filtration unit had a top chamber, a bottom chamber to collect filtered water, and a filter paper holding the unit between the two chambers. The filter paper was cut in the form of 4.5 cm circular discs. 2 filter papers of 0.21 mm thickness were placed on a support and were inserted into the paper holding unit. The top chamber had a capacity of 500 ml and the bottom chamber had a capacity of 1 L. 500 ml of model water containing the microspheres was fed into the top chamber. This water was allowed to pass through the filter paper and the filtrate was collected in the bottom chamber. The flow rate was measured as the time required to filter 500 ml of the input water and was found to be between 60-65 ml/min. The filtered water collected was analyzed for the removal of the microspheres.

For the filtration experiments using polyester fabrics, a set up similar to Tarson's filtration unit (having 10 L capacity and made of acrylic) was used. Fabrics were placed inside the fabric holding assembly and water containing the microspheres was passed through the fabric layers. The input and output water were tested to determine the microsphere removal.

Surface Charge

The model colloids and the collector media used in the experiments were characterized in terms of its surface charge. The surface charge of the Whatman filter paper was measured using Zeta Potential Analyzer Zeta Plus^{TM}, supplied by Brookhaven Instruments Corporation, USA, at an applied voltage of 100 V. For the Whatman filter paper, the paper was cut into small sizes and ground to get fine particles. A small aliquot (~30 ml) of the stock particle suspension was fed into the sample cell to measure the zeta potential. The sample cell consisted of two electrodes, an anode & a cathode. Molybdenum was used as an anode and placed at the left side and a Platinum rod was used as a cathode and placed at the right side of the cell. The cathode and the anode were inserted into the sample cell and connected to the zeta meter. The required voltage was applied and the electrodes were energized. As a result of this voltage, the particles, being negatively charged, moved towards the anode. The motion of the particles between the grid lines were tracked using a microscope kept above the sample cell and the zeta potential was noted.

Analysis of Microspheres

Polystyrene latex particles (microspheres) with an average size of 3 μ were used. The initial and final counts were determined by filtering diluted solution through a 0.45 μm Millipore filter paper. The microspheres were counted using an Olympus BX40 Optical Fluorescent Microscope.

Surface Morphology

A 1 cm x 1 cm sample was cut without disturbing the fiber and yarn alignment / arrangement within the fabric, mounted on a carbon tape and sputter coated with gold for 150 seconds. Images were collected using a Hitachi S-4700 model FESEM at 10Kv at different magnifications.

Surface Roughness

The topography and surface roughness of the substrates were characterized using a tapping mode AFM (Nanoscope 1V from Veeco, U.S.A.). The scanning area was fixed to 10μ.

RESULTS AND DISCUSSION

Role of Flow Velocity on Detachment

Based on the theory explained in Section 2.1, the net adhesive force acting on a particle at various flow velocities was calculated using the theoretical force balance Eq. (10) and is plotted in *Figure 1a*. No effect on the particle adhesion was observed up to a flow velocity of 0.0005 m/s for a size range of 0.1 to 10 μm. This result could be due to the van der Waals force of attraction being significantly higher than the detachment forces (electrical double layer force and lift force). While the smaller sized particles (d_p < 0.5 μm) remained attached to the collector media, the increase in flow velocity beyond a certain limit increased the drag and lift forces acting on the particle and caused the particle detachment of larger sized particles (d_p>1 μm) from the collector surface.

Since the theory of particle attachment onto the cylindrical substrate predicted the removal of more than 1 μm particle beyond a flow velocity of 0.0005 m/s, Model water 1 was prepared with 3μ microspheres to validate the prediction. This water was passed through a 10 L capacity fabric holding unit. Two layers of fabric were placed one above the other in the fabric holding unit.

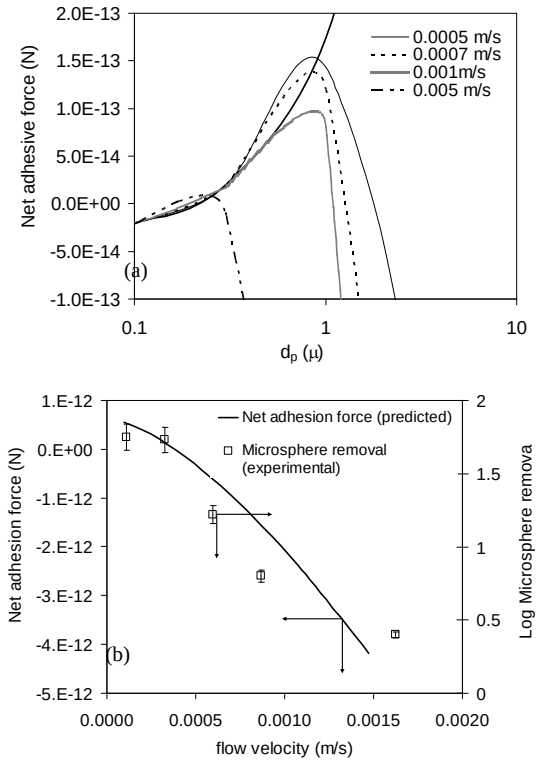

FIGURE 1. (a) Effect of flow velocity on net adhesion of particles on a cylindrical collector, (b) Effect of flow velocity on removal of 3 μm microspheres from a bed of fibrous media.

The throttle size was adjusted to give a water flow velocity in the range of 0.0001 to 0.002 m/s. The input and output water samples were collected and analyzed for microsphere removal. As shown in *Figure 1b*, it was experimentally confirmed that the higher flow velocities beyond 0.0005 m/s reduced the removal efficiency of the microspheres. All experiments were carried out 5 times and an average value has been plotted with a standard deviation. The net adhesive force was predicted for this system using Eq. (10) and the curve is plotted in *Figure 1b*. The predicted net adhesive force decreased with the increase in the flow velocities because of the lower adhesion due to the van der Waals force and higher lift force.

Role of Ionic Strength on Removal

To study the role of ionic strength on particle removal, Model water 1 was prepared with 3 μ microspheres. The experiments were conducted in the Tarson's filtration unit at 0.0005 m/s to prevent the detachment of microspheres due to high flow velocities. Sodium chloride or calcium chloride was used to vary the ionic strength between 0 to 100 mM. The results of the experiments are shown in *Figure 2a.*

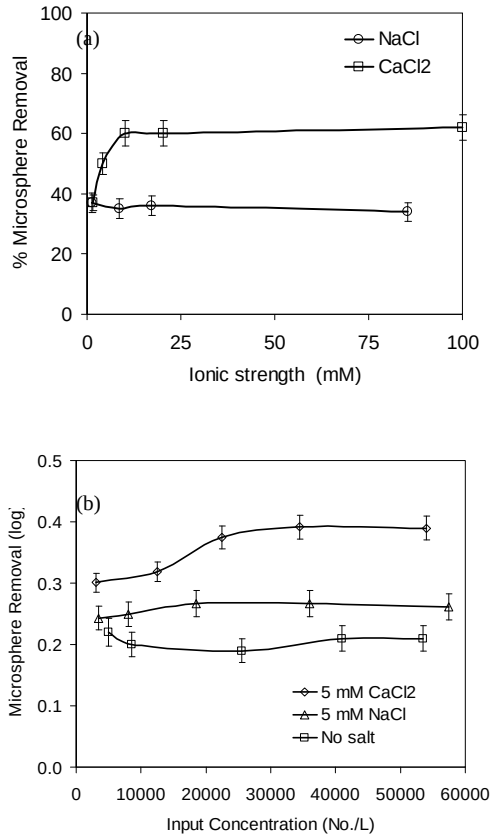

FIGURE 2. (a) Role of ionic strength on removal of microspheres from a bed of fibrous media, (b) Role of input concentration of the microspheres on removal in presence of sodium chloride and calcium chloride.

The values in the figures represent average values of 5 experiments with a standard deviation (in the range of 5-8%). The microsphere removal increased from 35% to 62% in case of calcium chloride. Addition of sodium chloride did not show any appreciable increase in microsphere removal and the removal remained constant at around 38% for the ionic strength range of 0 to 100 mM.

Role of Input Concentration on Removal

Experiments were conducted in the Tarson's filtration unit to demonstrate the effect of the concentration of microspheres on the removal and the result is shown in *Figure 2b*. The concentration of microspheres varied between 1000 to 60000 numbers/L. All experiments were carried out 5 times and an average value has been plotted with a standard deviation. In the absence of any salt, the microsphere removal was around 38% and independent of input concentration. In the presence of 5 mM of sodium chloride, the removal increased to 45% and was independent of input concentration. In the presence of 5mM of calcium chloride, the removal increased from 50 to 60% with an increase in the input concentration.

Surface Charge of Media and the Contaminants

The surface charge of the microspheres and fibers of the filter paper was measured using Zeta potential analyzer at various salt levels. *Table I* and *Table II* show the effect of ionic strength on the surface charge of the Whatman filter paper and the microspheres in the presence of sodium chloride and calcium chloride respectively.

TABLE I. Effect of ionic strength due to sodium chloride on the zeta potential of particle and media.

Ionic strength (mm)	Zeta potential (mV)	
	Whatman filter paper fibers	Microsphere
0	-37.7	-24.4
3.4	-36.1	-25.8
8.5	-37.7	-21.4
17.1	-38.2	-22
34.2	-38.1	-20.5
84.5	-37.9	-25.3

TABLE II. Effect of ionic strength due to addition of calcium chloride on the zeta potential of colloids and collector.

Ionic strength (mm)	Zeta potential (mV)	
	Whatman filter paper fibers	Microsphere
0	-37.7	-24.4
4	-32.7	-15.3
10	-31.8	-10.4
20	-19.1	-9.4
40	-17.6	-7.2
100	-15.2	-4.1

The increase in the ionic strength using sodium chloride did not affect the surface charge of the Whatman filter paper and microspheres. However, the increase in the ionic strength with calcium chloride increased the surface charge of the fiber and the microspheres dramatically. The charge of the microspheres and the fiber became relatively more positive and more microspheres stuck to the fiber.

DLVO Theory

The DLVO theory was used to explain the role of ionic strength on microsphere removal. The interaction energy profile for the microsphere-water-fiber system, based on DLVO theory and predicted using Eq. (12) and Eq. (13), is shown in *Figure 3.*

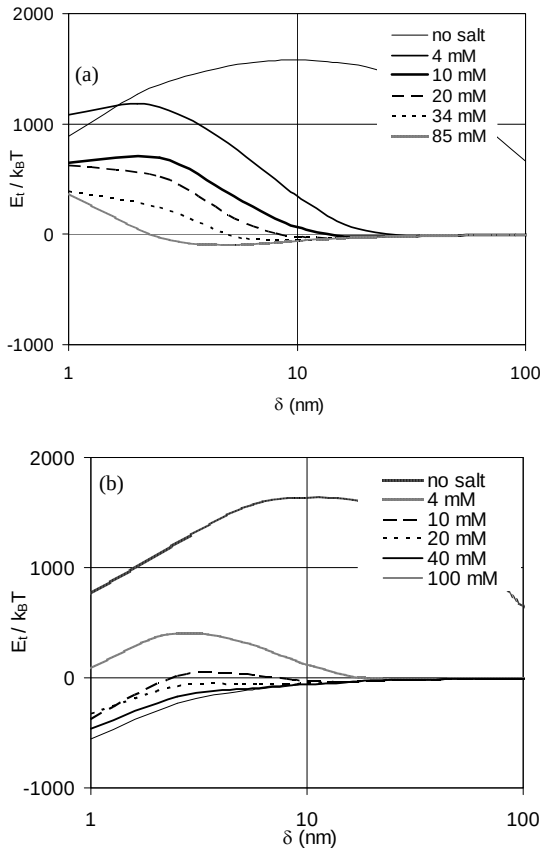

FIGURE 3. Calculated DLVO interaction energies for microsphere-fiber-water system as a function of separation distance: (a) in presence of Sodium chloride, (b) in presence of Calcium chloride.

The interaction profiles are based on the zeta potential values indicated in *Table I* and *Table II* and the Hamaker constant of 1 x 10^{-20} J for a latex-water-fiber system [1, 9]. The DLVO profile for microspheres reveals the existence of a significant energy barrier at an ionic strength between 1 to 20 mM in the presence of sodium chloride (*Figure 3a*). Specifically, the energy barrier for the microspheres varied from ~1600 k_BT, in the absence of any salt, to ~620 k_BT, using sodium chloride, and became negative using calcium chloride at ~ 20 mM (*Figure 3b*). These high energy barriers suggest that the microsphere deposition in the primary minima is highly unlikely. Even though, qualitatively, the DLVO theory predicts the reduction in the energy barrier with an increase in the ionic strength, the energy barrier for an ionic strength < 20 mM is a significant amount, for which the microsphere removal is not possible. However, as observed experimentally in *Figure 2a*, the microspheres were removed at an even lower ionic strength. Hence, DLVO theory alone is not sufficient to explain the phenomena of the removal of the microspheres on to the collector surface.

Role of Secondary Minima on Removal

The existence of secondary energy minima has been reported in the literature [1, 9, 10, 14] which occurs at a higher separation distance with respect to the collector surface. Based on the DLVO interaction profiles, the depth of the secondary minima was predicted at various salt levels and the data is reported in *Table III.* An increase in the ionic strength resulted in an increase in the depth of the secondary minima and its position came closer to the collector surface. Such interaction energy profiles suggest that microspheres can be captured in the secondary energy minimum. A microsphere will remain associated with the collector surface in this energy minimum unless it has sufficient energy to allow the microsphere to escape. The data in *Table III* also suggests that the depth of the secondary minima in the presence of calcium chloride is more than that of the sodium chloride. In the presence of calcium chloride, beyond 20 mM, the secondary minima did not exist and the microspheres entered into the favorable zone of chemical-colloidal interactions because there was no further increase in the removal.

TABLE III. Calculated secondary minimum depth and separation distance between collector surface and 3 μ microspheres as a function of solution ionic strength.

Ionic strength (mm)	Depth of secondary minima (KBT)		Secondary minima separation distance (nm)	
	Using NaCl	Using $CaCl_2$	Using NaCl	Using $CaCl_2$
4	-12	- 12	40	30
10	-23	-23	30	15
20	-34	-34	15	6
40	-55	-55	8	ND*

(ND* = No secondary minima)

Modified DLVO Theory: Role of Surface Roughness on Removal

DLVO theory does not take into account the effects of the surface roughness and charge heterogeneity on the collector and the particle or microsphere which significantly impacts the predictability. To confirm the existence of the rough surface on the fiber, SEM images of the fibers were taken for the Whatman filter paper and the polyester fabric. *Figure 4* shows SEM image of the Whatman filter paper and nonwoven fabric which confirmed the presence of the rough surface on the fiber.

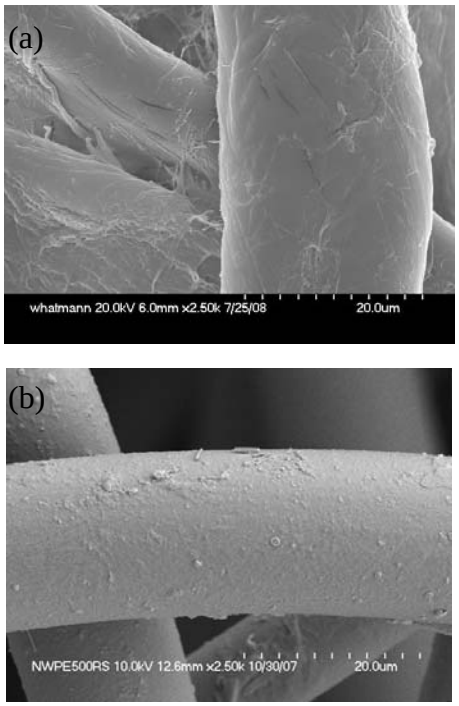

FIGURE 4. Scanning electron microscopy of (a) Whatman filter paper and (b) nonwoven polyester.

The surface roughness of the fabric samples was measured using an AFM technique. *Figure 5* shows the AFM images of the Whatman filter paper. It was found the RMS roughness of the Whatman filter paper was in the order of 80-100 nm. The energy of the interaction between a microsphere (in DI water in the absence of any added salt) and a collector for different values of the surface roughness in the range of 10 to 100 nm was predicted using Eq. (13) and Eq. (22). The result is shown in *Figure 6a*. It was found that the surface roughness of 100 nm alone predicted a reduction in the energy barrier from ~1630 to ~290 k_BT in the absence of any salt. *Figure 6b* shows the effect of the addition of calcium chloride on the predicted interaction profile. The presence of calcium chloride along with the surface roughness predicted a significant reduction in the energy barrier even at lower ionic strengths, thus explaining the higher removal of microspheres in the presence of calcium chloride.

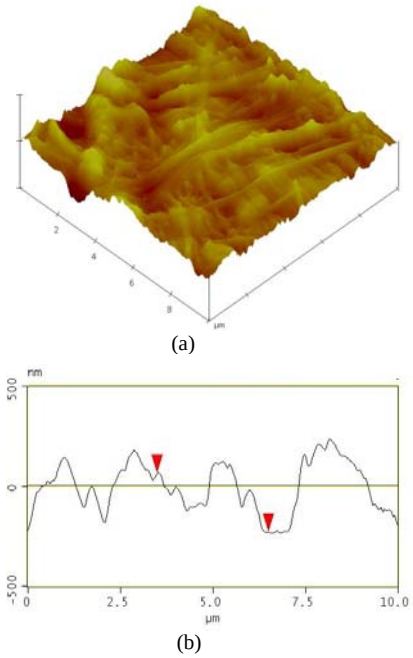

FIGURE 5. Surface roughness as measured by AFM technique for Whatman filter paper (a) 3D image, (b) 2D image

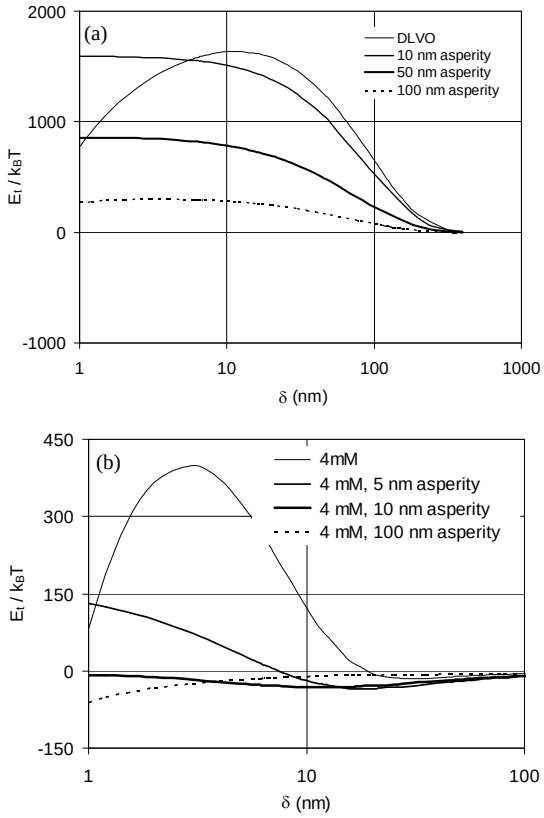

FIGURE 6. Calculated DLVO interaction energies for microsphere-fiber-water system as a function of separation distance due to surface roughness: (a) In absence of any added salt (b) in presence of 4 mM Calcium chloride.

Modified DLVO Theory: Role of Charge Heterogeneity on Removal

The energy of interaction between a microsphere (in DI water in the absence of any added salt) and a collector for different values of charge heterogeneity in the range of 0 to 20 mV was predicted using Eq. (12) and Eq. (24). The result is shown in *Figure 7*.

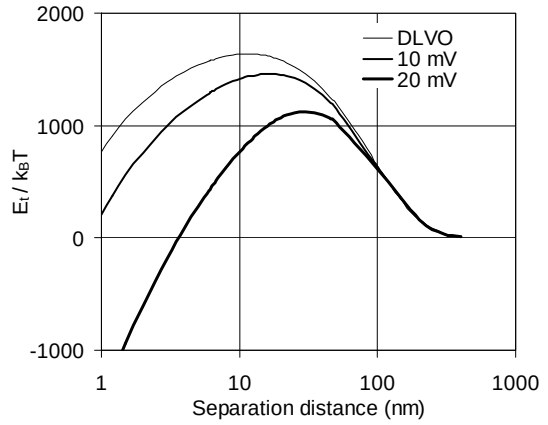

FIGURE 7. Predicted energy profiles for microsphere-fiber-water system in presence of charge heterogeneity of collector and microspheres without any added salt.

It was predicted that even with a heterogeneity as high as 20 mV, the energy barrier was reduced from ~1600 to 1100 k_BT. Hence, the extent of the energy variation of interaction, with respect to the change in charge heterogeneity, appeared very minimal. A similar variation in the reduction of the energy barriers can be predicted at higher ionic strengths for the microsphere-fiber system. Based on *Figures 3 and 5*, it can be concluded that the contribution of the surface roughness was more prominent compared to the charge heterogeneity.

CONCLUSIONS

The role of flow velocity, colloid concentration and ionic strength on colloid adhesion onto a cylindrical collector was studied in this work. Microspheres were used as the model colloids and the Whatman filter paper and nonwoven fabric were used as the model collectors. The existing theory on particle attachment was modified to take into account the lift and Brownian diffusive forces. The surface roughness and charge heterogeneity in DLVO theory accounted for better predictability of colloid removal. The following conclusions can be made based on the findings:

1. High flow velocities predicted the detachment of the larger sized particles due to higher lift forces. This theory was validated by using microspheres of 3 µm which showed a decrease in the removal efficiency at higher flow velocities.
2. The addition of calcium chloride caused a significant improvement in the colloid removal compared to sodium chloride at similar ionic strengths. The increase in the removal was due to an increase in the zeta potential of the fiber and colloids (surface charge became relatively more positive), a reduction in the energy barrier of interaction, the deposition in the secondary minima, the roughness and charge heterogeneity of the fiber and colloids.
3. An increase in the concentration of the microspheres showed a marginal improvement on the removal in the presence of calcium ions.
4. DLVO theory alone could not predict the effect of the ionic strength on the adhesion of particles and microspheres. The observed discrepancy between theory and experimental results came down to the incorporation of the surface roughness and charge heterogeneity of the colloid and collector.
5. The surface roughness contributed more significantly to the colloid removal compared to the charge heterogeneity.

NOMENCLATURE

A	area of parallel plates
C_0	influent concentration at the entry of the packed bed.
C	effluent concentration at the exit of the packed bed
d	diameter of the collector
d_p	diameter of the colloidal particle
e	charge of the electron
E_{vdw}	interaction potential due to van der Waals forces
E_{EDL}	interaction potential due to electrical double layer repulsion force
E_{DLVO}	Total energy of interaction based on DLVO calculations
$E_T(\delta)$	The total interaction energy between a single particle and a single half-sphere protrusion
F_{adh}	force of adhesion for a spherical particle interacting with a surface having an asperity
f	bed porosity
F_L	London-van der Waals force
F_D	Electrical double layer force
F_d	Hydrodynamic Drag force
F_l	Hydrodynamic Lift force
F_F	Frictional force
F_G	Gravity force
F_B	Buoyancy force

F_b Brownian force
F_{Adh} Net adhesive force
L depth of bed
H Hamaker constant
K Debye reciprocal double layer thickness
k_B Boltzmann's constant
k_f coefficient of sliding friction
k'_f proportionality constant
$n_{i\infty}$ bulk number density of ions in solution
r_a radius of asperity
r_p radius of colloidal particle
r_c collector radius
S specific surface area of the deep bed filter, defined as the surface area per unit filter bed volume
T absolute temperature
u_p particle velocity
u approach fluid velocity
y_{max} height of asperity
z valence of the ion species

GREEK SYMBOLS

τ_w shear stress acting on the collector
μ fluid viscosity
α collision efficiency factor (sticking coefficient)
η single collector efficiency
δ separation distance between the particle and the collector plane
ε_0 dielectric constant (permittivity) in vacuum
ε relative dielectric constant of the fluid
ζ_p zeta potential of the particle
ζ_g zeta potential of the collector
ξ non dimensional gap defined as ratio of separation distance between particle and collector and particle radius
ρ fluid density
φ reduced potential of either the collector or the particle

REFERENCES

[1] Elimelech, M.; O'Melia, C.R.; Kinetics of Deposition of Colloidal Particles in Porous Media; *Environ. Sci. & Technol*. 1990, *24*, 1528-1536.

[2] Li, Y; Park, C. W.; Prediction of mass transfer rate in fibrous and granular media using packing permeability; *J. Coll. Interf. Sci*. 1997, *185*, 49-53.

[3] Redman, J. A; Walker, S. L.; Elimelech, M.; Bacterial Adhesion and Transport in Porous Media: Role of the Secondary Energy Minimum; *Environ. Sci. and Technol.* 2004, *38*, 1777-1785.

[4] Yao, K. M.; Habibian, M. T.; O'Melia, C. R.; Water and waste water filtration: concepts and applications; *Environ. Sci. Technol*. 1971, *5(11)*, 1105-1111.

[5] Logan, B. E.; Hilbert, T. A.; Arnold, R. G.; Removal of bacteria in laboratory filters: models and experiments; *Wat. Res*. 1993, *27(6)*, 955-962.

[6] Logan, B. E.; Jewett, D. G.; Arnold, R. G.; Bouwer, E. J.; O'Melia, C. R.; Clarification of clean-bed filtration models; J. Environ. Eng. 1995, 869-873.

[7] Bai, R.; Tien, C.; Particle detachment in deep bed filtration; *J. Coll. Interf. Sci*. 1997, *186*, 307-317.

[8] Truesdail, S. E.; Lukasik, J.; Farrah, S. R.; Shah, D. O.; Dickinson, R. B.; Analysis of bacterial deposition on metal (hydr)oxide-coated sand filter media; *J. Coll. Interf. Sci*. 1998, *203*, 369-373.

[9] Elimelech, M.; O'Melia, C. R.; Effect of Particle Size on Collision Efficiency in the Deposition of Brownian Particles with Electrostatic Energy Barriers; *Langmuir* 1990, *6*, 1153-1163.

[10] Song, L.; Johnson, P. R.; Elimelech, M.; Kinetics of Colloid Deposition onto Heterogeneously Charged Surfaces in Porous Media; *Environ. Sci. & Technol.* 1994, *28(6)*, 1164-1171.

[11] Tufenkji, N.; Elimelech, M.; Breakdown of Colloid Filtration Theory: Role of the Secondary Energy Minimum and Surface Charge Heterogeneities, *Langmuir* 2005, *21*, 841-852.

[12] Rabinovich, Y. I.; Adler, J. J.; Ata, A.; Singh, R. K.; Moudgil, B. M.; Adhesion between nanoscale rough surfaces: 1. Role of asperity geometry; *J. Coll. Interf. Sci*. 2000, *232*, 10-16.

[13] Rabinovich, Y. I.; Adler, J. J.; Ata, A.; Singh, R. K.; Moudgil, B. M.; Adhesion between nanoscale rough surfaces: 2. Measurement and comparison with theory; *J. Coll. Interf. Sci*. 2000, *232*, 17-24.

[14] Katainen, J.; Paajanen, M.; Ahtola, E; Pore, V; Lahtinen, J; Adhesion as an interplay between particle size and surface roughness; *J. Coll. Interf. Sci*. 2006, *304*, 524-529.

[15] Suresh, L.; Walz, J. Y.; Effect of surface roughness on the interaction energy between a colloidal sphere and a flat plate; *J. Coll. Interf. Sci*. 1996, *183*, 199-213.

[16] Suresh, L.; Walz, J. Y.; Direct measurement of the effect of surface roughness on the colloidal forces between a particle and flat plate; *J. Coll. Interf. Sci*. 1997; 196, 177-190.
[17] Velegol, D; Thwar, P. K.; Analytical model for the effect of surface charge non-uniformity on colloidal interactions; *Langmuir* 2001, *17*, 7687-7693.

AUTHORS' ADDRESSES
Manoj Dagaonkar, Ph.D.
Udayan Majumdar
Hindustan Unilever Limited
64, Main Road, Whitefield
Bangalore, Karnataka 560066
INDIA